IEEE Access
Multidisciplinary : Rapid Review : Open Access Journal

Received 31 July 2024, accepted 6 August 2024, date of publication 13 August 2024, date of current version 2 September 2024.

Digital Object Identifier 10.1109/ACCESS.2024.3443066

RESEARCH ARTICLE

Enhancing Classification Accuracy of fNIRS-BCI for Gait Rehabilitation

HAMZA SHABBIR MINHAS[1], HAMMAD NAZEER[1], (Senior Member, IEEE), NOMAN NASEER[1], (Senior Member, IEEE), UMAR SHAHBAZ KHAN[2,3], (Member, IEEE), ALI R. ANSARI[4], AND RAHEEL NAWAZ[5]

[1]Department of Mechatronics and Biomedical Engineering, Air University, Islamabad 44000, Pakistan
[2]Department of Mechatronics Engineering, National University of Sciences and Technology, Islamabad 44000, Pakistan
[3]National Centre of Robotics and Automation (NCRA), Rawalpindi 46000, Pakistan
[4]Department of Mathematics and Natural Sciences, Gulf University for Science and Technology, Mishref Campus, Hawally 32093, Kuwait
[5]VC Office, Staffordshire University, ST4 2DE Stoke-on-Trent, U.K.

Corresponding author: Noman Naseer (noman.naseer@au.edu.pk)

This work was supported in part by the Gulf University for Science and Technology.

This work involved human subjects or animals in its research. Approval of all ethical and experimental procedures and protocols was granted by the Ethical Committee, Air University under Approval No. AU/EA/2021/03/002, and performed in line with the Declaration of Helsinki.

ABSTRACT To improve mobility and rehabilitation, precise and adaptive control mechanisms have been developed for lower limb exoskeletons. Brain-computer interface (BCI) provides advanced and intuitive control of assistive and rehabilitation exoskeletons to aid the user. Functional near-infrared spectroscopy (fNIRS) is a non-invasive, and portable brain imaging modality, gained momentum in rehabilitation studies in the last decade. This study provides a novel approach to control a lower limb exoskeleton with enhanced classification accuracy using fNIRS-based BCI, the k-nearest neighbors (kNN) classifier, and optimal feature combination. The brain signals were acquired using fNIRS for walking vs rest for twenty healthy participants, having ten trials for each participant. The statistical measures: mean, peak, variance, skewness, kurtosis, and slope are extracted as features. Optimal feature combination was analyzed and selected for enhanced classification accuracy. kNN was analyzed and selected as an optimal classifier with optimal 'k' (number of nearest neighboring data points that the kNN considers while classifying a new data point) using elbow method to improve classification performance. The proposed method achieves an average classification accuracy of 88.19 ± 2.55 %, in offline configuration. In order to control exoskeleton in online settings, simulated online classification was performed using one unknown trial, fed as real-time signal. Sliding window of 2.5 sec is used and achieved average classification accuracy of 97.5%. This research represents a major advancement in user-centric assistive technologies and advances the field of neuro-powered exoskeletons. It also lays the groundwork for future advancements in the integration of neuroimaging, machine learning, and rehabilitation.

INDEX TERMS Brain–computer interface, functional near-infrared spectroscopy, gait cycle, lower limb exoskeleton, rehabilitation.

I. INTRODUCTION

Human gait is a fundamental human activity that involves coordination among various parts of the brain, muscles, and limbs. Signals from the brain's sensory and motor areas trigger the activation of premotor and supplementary motor areas of the cerebral cortex [1]. Globally, walking disabilities continue to be a major cause resulting in improper gait patterns. Gait impairment is the leading cause of reduced independence in daily activities for patients. Moreover, gait rehabilitation often faces challenges in achieving a fully restored gait pattern [2], [3]. A significant amount of

The associate editor coordinating the review of this manuscript and approving it for publication was Shovan Barma.

scientific work has been done in the recent decade into creating technologies that can assist physiotherapists in their work; some of these devices support a patient's body weight, and patients are asked to practice walking on a treadmill or other specially designed platforms [4]. While such methods cannot fully restore a physiological gait pattern, but it can enhance the independence of stroke patients, particularly those with limited motor function. Most patients only show signs of walking ability recovery in 50% to 60% of cases [5], [6]. Even though some patients are able to walk on their own, their abnormal gait makes it difficult for them to carry out daily tasks and increases their risk of injury [7], [8].

Top-down approaches involving brain-computer interfaces (BCIs) that control external devices through metabolic brain activity could be a viable way to influence motor behavior and brain reorganization in patients [9]. BCI is a neurotechnology that shows great promise in improving the daily lives of individuals with neuromuscular conditions caused by stroke, spinal cord injuries and amyotrophic lateral sclerosis (ALS) [8], [10]. The essential elements of a BCI robotic system include brain activation patterns specific to tasks, brain data collection, machine learning tools for decoding brain signals and the use of control/feedback devices [11]. Successful motor rehabilitation is often linked to restoring activity in the brain regions surrounding the lesion (perilesional areas) and promoting stimulation in these areas [12]. BCI training, which reinforces activity in these perilesional areas, has shown positive results in motor rehabilitation. Electroencephalographic signals were used by the majority of BCIs designed for motor rehabilitation to power prosthetics that facilitate upper limb movement [13]. Nevertheless, only a small number of BCI systems were developed to control lower limb exoskeletons. Functional near-infrared spectroscopy (fNIRS) is a non-invasive optical imaging method that can be used to acquire signals from brain for the rehabilitation of lower limb movement [14], [15]. fNIRS is a promising method in BCI research that offers multiple advantages over other neuroimaging techniques like enhanced safety and portability [16], [17].

Conventional methods of controlling exoskeletons involve acquiring signals using electromyography (EMG). However, these methods often lack the adaptability required for seamless integration into a variety of settings. Conventional control paradigms are challenged by real-time adaptations to user's intent, terrain changes, or variations in walking speed [18]. This novel combination of neuroimaging and robotics has the potential to transform mobility assistance and rehabilitation techniques while also improving the natural interaction between users and their exoskeletons. A paradigm shift has occurred with the integration of fNIRS into the exoskeleton control architecture. fNIRS is employed to measure changes in the blood oxygenation levels as indicators of brain activity, facilitating the development of BCI [19]. Compared to other non-invasive BCI modalities such as functional magnetic resonance imaging (fMRI) and electroencephalography (EEG), fNIRS is used due to its affordability, portability, and safety in optical brain imaging [20]. These advantages make fNIRS a valuable tool for BCI systems, enabling control and operation of external devices through brain signals [21]. A more sophisticated comprehension of user intent and cognitive engagement during locomotion is made possible by fNIRS, which decodes brain signals associated with changes in the lower limb [22]. There are several advantages to real-time control of exoskeletons using fNIRS [23], [24]. This approach, which relies on the user's neural activity for control, facilitates a more intuitive and natural interaction between the user and the exoskeleton. This improved synchronization between the user's intentions and the exoskeleton's actions can reduce cognitive load [10], [11]. Furthermore, fNIRS-based exoskeleton control could be used to enhance a healthy person's physical capabilities for activities requiring more strength or endurance [20], [22].

This paper presents an approach for enhancing classification accuracy for gait rehabilitation by selecting optimal feature combinations. kNN was selected as an optimal classifier and value of 'k' was determined using elbow method to enhance the classification accuracy without overfitting. In order to control exoskeleton in online settings, simulated online classification was performed in MATLAB® and control commands were generated. This approach provides a robust framework for refining gait rehabilitation techniques and advancing the efficacy of exoskeleton control in practical applications. Fig. 1 represents a schematic flowchart of the research.

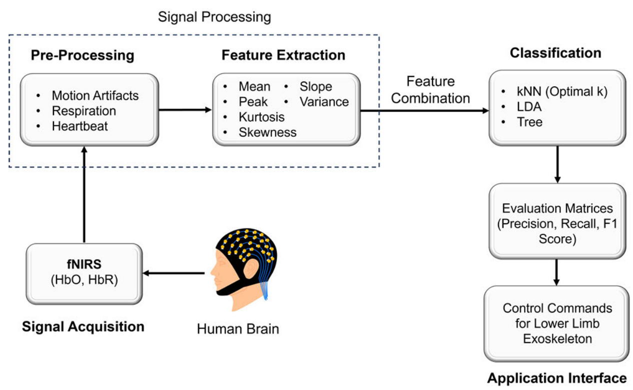

FIGURE 1. Schematic flowchart of research.

II. MATERIALS AND METHODS

A. SUBJECTS

Twenty young and healthy participants with an average age of 22.5 years were included in the study. It was made sure that none of the participants had any major medical illness like cardiovascular, neurological or visual disorder [26] because cardiovascular diseases alter brain blood flow regulation, while neurological disorders may affect neural activation patterns during tasks [27]. The experiment was approved by the Ethical Committee, Air University under approval number AU/EA/2021/03/002. The experiment was performed according to principles mentioned in the Declaration of Helsinki to emphasize on privacy protection and well-being of the participant [28]. Before data acquisition, each participant provided written consent after receiving a detailed explanation about the research.

B. DATA ACQUISITION

Optodes are components that emit and detect near-infrared light to measure changes in hemoglobin concentrations in the brain. Source optodes (high-powered dual 32mW LEDs) are responsible for emitting near-infrared light into the scalp while detector optodes are used to detect the light that has traveled through the brain tissue and has been scattered back to the surface. The precise positioning of the optodes is important in fNIRS studies as it affects the quality of the acquired signal [29]. A network of 20 channels using 8 sources and 8 detector pairs was established. A fixed distance of 3 cm was kept between both sources and detectors to minimize variability and ensure accurate measurement of hemodynamic responses within specific areas of the brain [26], [30]. Data was recorded using continuous-wave NIRSport2 fNIRS system and Aurora Software made by NIRx Medical Technologies, Germany. Accurate event markers were generated using PsychoPy software which were synchronized with the experimental paradigm to correlate neural responses with specific experimental triggers. Improper attachment of optodes to the head and optical interference caused by dense hair can affect the fNIRS signals [31], [32]. Therefore, it is recommended to wash the hair before the experiment to avoid interference due to oil and dandruff. Position of optodes were aligned according to the EEG 10-20 system [16], [33]. The motor montage was designed in view of the previous literature [34]. The red circles represent the location of source while blue circles represent the detectors. To gain a visual understanding of where the optodes were placed in the motor cortex area of the brain, please refer to Fig. 2.

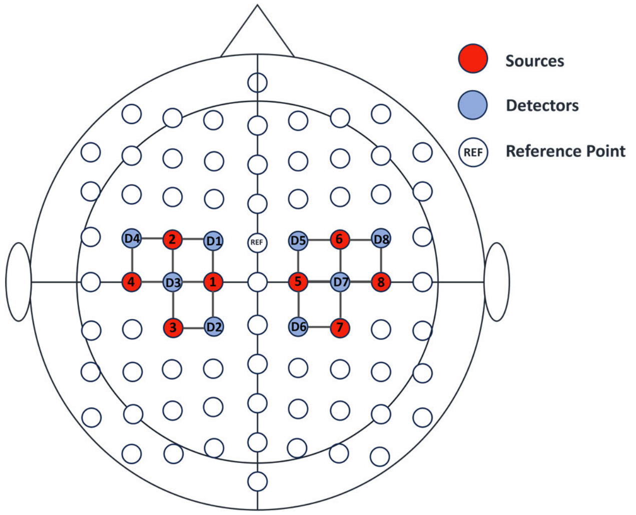

FIGURE 2. Optodes placement on the motor cortex region of the brain. 20 channels were used to record brain signals with a setup of 8 emitters and 8 detectors positioned 3 cm from each other.

C. EXPERIMENTAL PARADIGM

The trial began with participant standing on a treadmill positioned in front of a computer screen 2 meters away. Before starting, detailed instructions on the entire process were provided. Participants were asked to relax and get ready for the upcoming tasks. The experiment was performed in a dark room to avoid light interference. A 30-second rest was given initially to establish accurate baseline measurements allowing their body's hemodynamic response to stabilize to establish a stable baseline of hemodynamic activity before any stimuli were introduced [35]. This baseline serves as a reference against which changes in blood flow can be measured during stimuli. During this time, participants were encouraged to stay still without making any deliberate movements. After the initial rest period, a 20-second walking task was performed where participants were instructed to focus on maintaining a proper gait cycle on the treadmill. This was followed by a 20-second rest period provided for participants to recover and prepare for the next activity. This cycle of physical activity and rest was repeated ten times in total. Finally, there was a concluding 30-second rest period given to allow participants to return to their normal state. Fig. 3 provides an illustration of the experimental paradigm and Fig. 4 gives a view of the experimental setup. To ensure accurate and consistent data among all participants, explicit instructions were given not to make unnecessary physical movements or gestures that could introduce noise or artifacts into the collected data.

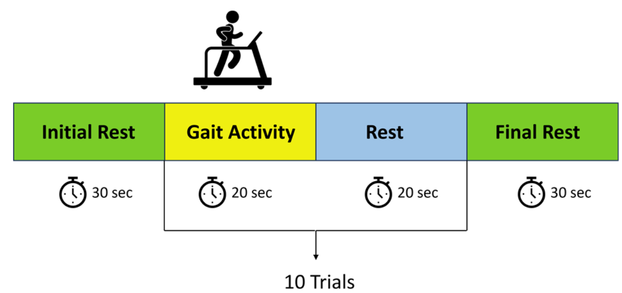

FIGURE 3. Schematic representation of the experimental paradigm.

D. DATA PREPROCESSING

The data preprocessing for the study involved using the Satori 2.0 software developed by NIRx Medical Technologies, Germany. Initially, the raw data was imported, and the necessary procedures and computations were performed to process and analyze it. In fNIRS studies, data collected from different channels often contains noise and artifacts caused by factors like subject movement, respiration (around 0.3 Hz), heartbeat (around 1.0 Hz), and mayer waves [36]. Butterworth filter was applied with a range of 0.01 Hz to 0.3 Hz to remove physiological noises [37], [38]. Butterworth filter is preferred because it can ensure a consistent frequency

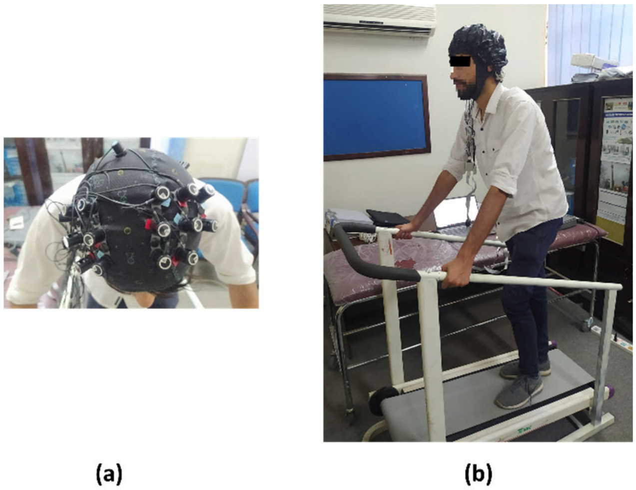

FIGURE 4. **(a) Montage of 8 × 8 with optodes placed on motor cortex region of the brain; (b) Experimental setup with participant walking on treadmill.**

response within the desired range while effectively reducing frequencies outside that range [39].

Following the filtration process, the modified Beer-Lambert Law was applied to figure out how much oxyhemoglobin (ΔHbO) and deoxyhemoglobin (ΔHbR) changed [40], [41]. Using equation (1), the changes in ΔHbO and ΔHbR concentrations can be measured precisely, providing insight about the biochemical makeup of the of brain tissues under consideration.

$$\begin{bmatrix} \Delta[HbO]_t \\ \Delta[HbR]_t \end{bmatrix} = \frac{\begin{bmatrix} \sigma_{HbO}(\varphi_1) & \sigma_{HbR}(\varphi_1) \\ \sigma_{HbO}(\varphi_2) & \sigma_{HbR}(\varphi_2) \end{bmatrix}^{-1} \begin{bmatrix} \frac{\Delta O_D(t,\varphi_1)}{\Delta O_D(t,\varphi_2)} \end{bmatrix}}{Lxd} \tag{1}$$

where, $\sigma_{HbO}(\varphi)$ and $\sigma_{HbR}(\varphi)$ are the extinction coefficients of ΔHbO and ΔHbR in the units of $\mu M^{-1}cm^{-1}$ respectively, d is the differential path length factor, $\Delta O_D(t, \varphi_j)$ is the optical density change of light, and L is the emitter-detector distance measured in mm.

E. ACTIVATION MAPS

The brain activation maps were generated using Satori 2.0 software to visualize cognitive activity in different regions of the brain. Brain activation refers to changes in ΔHbO levels detected by sensors observed from the beginning to the end of a trial. Fig. 5 displays views of brain activation regions for a single participant observed during activities associated with the gait cycle for a single subject. These activation regions hold importance as they reveal the specific areas of the brain that are engaged and more active when the subject walks. By comprehending these activated regions, brain regions responsible for controlling and coordinating movement throughout the walking process can be identified. During a gait cycle, primary sensorimotor cortex, thalamus, and basal ganglia appeared to be more activated which are in accordance with previous literature [42], [43].

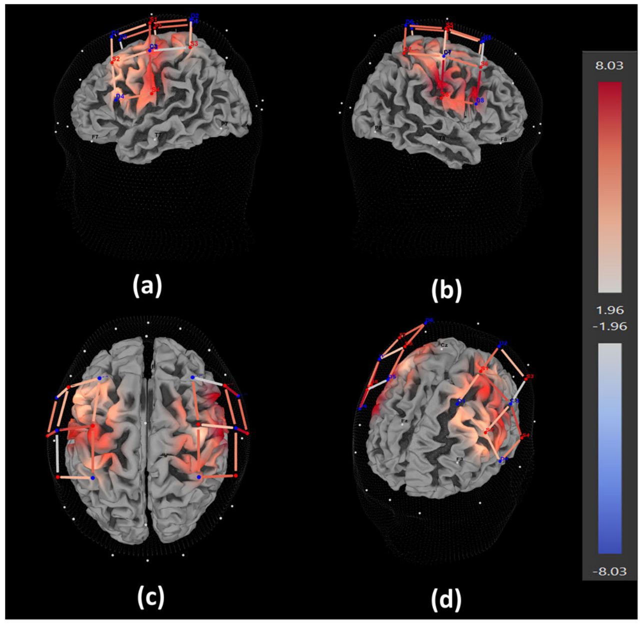

FIGURE 5. **Brain activation maps for gait activity with respect to rest generated using Satori 2.0. a) Left View, b) Right View, c) Top View, d) 3D View.**

This information provides insights into how our brains function and coordinate movements, which is beneficial for research on motor control, rehabilitation, and understanding neurological conditions that impact walking abilities [44], [45].

F. FEATURE EXTRACTION

The data analysis involved extracting statistical features like mean, peak, skewness, variance, slope, and kurtosis using ΔHbO. A comparison was conducted with varying feature combinations as three-, four-, five-, and six-feature combinations to achieve the optimal accuracy. The classifiers used were K nearest neighbors (kNN), Linear Discriminant Analysis (LDA), and Tree classifier. Calculations for all six features were done as follows:

$$Mean = \frac{1}{N}\sum\nolimits_{j=1}^{N} S_j \tag{2}$$

where N is the total number of observations and S_j shows the ΔHbO value across each observation. Variance was calculated as:

$$Variance = \frac{1}{N-1}\sum\nolimits_{k=1}^{N-1} (S_k - \mu) \tag{3}$$

where S_k is the input signal, N is the number of samples, and μ is the computed mean value. Skewness is the measure of asymmetry in the distribution, while kurtosis focuses on the shape of the distribution's tails, whether they are more peaked or spread out. Skewness and kurtosis can be computed as:

$$Skewness(S) = E_x\left(\frac{S-\delta}{\sigma}\right)^3 \tag{4}$$

$$Kurtosis(S) = E_x\left(\frac{S-\delta}{\sigma}\right)^4 \tag{5}$$

where E_x is the expected value of S and σ is the standard deviation of S. The slope was calculated using the *polyfit* function in MATLAB®. This function fits a line to the provided data points. To find the maximum signal value (peak), the *max* function in MATLAB® was employed.

G. OPTIMAL VALUE OF K

kNN is a machine learning algorithm that can be applied to tasks involving classification. The value of 'k' represents the number of nearest neighbors considered in the analysis. For classification of a new data point, the kNN algorithm determines the nearest neighbors based on a distance measured [46]. The selection of the optimal value of 'k' is important in determining the performance of the kNN algorithm [47]. Selecting an appropriate value of 'k' in the kNN classifier is crucial for classification accuracy and control command generation. Smaller value of 'k-nearest neighbors' can make the algorithm too sensitive to noise [48], causing inconsistent commands. On the other hand, a large 'k-nearest neighbors ' can smooth out important details, leading to less responsive control. Therefore, choosing an appropriate value of 'k' ensured that the exoskeleton responded promptly to the user's movements. To identify the optimal 'k' value, the elbow method is employed. This method plots the performance metrics of the data against different 'k' values and determining the point where precision increases [49]. Value of 'k' can be given as:

$$k = \sqrt{\frac{N}{2}} \tag{6}$$

where 'N' stands for the number of samples in the training dataset. For training and testing the dataset through ten trials, a 10-fold cross-validation technique was applied. It means that for each trial, one of the 10 folds were used as validation dataset while the remaining nine folds were used for training.

III. RESULTS

A. FEATURE COMBINATION

All possible feature combinations of three, four, five, and six features were extracted using ΔHbO for twenty participants. An analysis was performed on all possible feature combinations to identify the one that yielded the highest classification accuracy. Six-feature combination (mean-peak-variance-skewness-kurtosis-slope) provided significantly better classification accuracies as compared to the other feature combinations which was verified by Student's t-test ($p < 0.0141$). Table 1 presents the accuracy of each classifier for all feature combinations on the dataset. Fig. 6 illustrates the graphical comparison, highlighting the best-performing classifier, which is kNN with an average accuracy of $88.19 \pm 2.55\%$. A student's t-test (p-value) was performed to determine the significant difference between the mean values of results of classification accuracies [50]. kNN performed significantly better than other classifiers, therefore, a student's t-test was performed to indicate statistical significance by comparing the results of kNN with LDA and Tree classifier. The values of both student's t-tests were less than 0.05 i.e., $p < 0.0141$ for Tree and $p < 1.6 \times 10^{-38}$ for LDA which shows that results are unlikely to have occurred under the assumption.

TABLE 1. Average classification accuracies of 20 subjects across multiple feature combinations.

Feature Combination	Accuracy (%)		
	KNN	LDA	Tree
Mean Peak Variance	85.75	75.24	83.75
Mean Peak Slope	87.71	76.17	86.95
Mean Peak Skewness	86.22	75.35	84.14
Mean Peak Kurtosis	84.29	74.21	83.01
Mean Variance Skewness	87.49	75.23	87.33
Mean Variance Kurtosis	86.25	74.18	86.06
Mean Variance Slope	89.33	76.27	88.93
Mean Skewness Kurtosis	85.42	74.08	83.61
Mean Skewness Slope	88.99	76.22	88.37
Mean Kurtosis Slope	88.07	75.23	87.57
Peak Variance Skewness	87.03	74.39	86.28
Peak Variance Kurtosis	84.92	71.45	83.90
Peak Variance Slope	87.89	74.36	87.28
Peak Skewness Kurtosis	84.34	71.59	82.79
Peak Skewness Slope	88.15	74.17	87.30
Peak Kurtosis Slope	86.71	71.89	85.73
Variance Skewness Kurtosis	80.68	65.64	79.14
Variance Skewness Slope	84.52	68.59	84.17
Variance Kurtosis Slope	82.92	64.24	81.93
Skewness Kurtosis Slope	81.97	66.87	80.32
Mean Peak Variance Skewness	88.38	75.44	88.22
Mean Peak Variance Kurtosis	87.35	75.19	87.99
Mean Peak Variance Slope	90.58	77.22	90.36
Mean Peak Skewness Kurtosis	87.86	75.40	87.28
Mean Peak Skewness Slope	90.89	77.11	90.62
Mean Peak Kurtosis Slope	90.03	76.12	90.20
Mean Variance Skewness Kurtosis	89.27	75.36	89.68
Mean Variance Skewness Slope	91.71	77.04	92.33
Mean Variance Kurtosis Slope	91.15	76.48	91.80
Mean Skewness Kurtosis Slope	90.78	76.33	90.59
Peak Variance Skewness Kurtosis	88.73	74.71	88.86
Peak Variance Skewness Slope	91.10	76.29	91.29
Peak Variance Kurtosis Slope	90.79	74.29	90.51
Peak Slope Kurtosis Slope	90.18	74.64	89.80
Variance Skewness Kurtosis Slope	86.00	68.77	87.23
Mean Peak Variance Skewness Kurtosis	89.07	75.47	89.96
Mean Peak Variance Skewness Slope	91.80	77.32	92.34
Mean Peak Variance Kurtosis Slope	90.79	77.20	92.05
Mean Peak Skewness Kurtosis Slope	91.18	77.15	91.89
Mean Variance Skewness Kurtosis Slope	92.00	77.25	93.01
Peak Variance Skewness Kurtosis Slope	92.32	76.58	92.33
Mean Peak Variance Skewness Kurtosis Slope	93.50	77.30	92.95

The confusion matrix plays a vital role in evaluating the performance of a classification model, especially when it comes to distinguishing between walking and rest activities. It helps us understand how well the model correctly categorizes instances into their respective classes. The real importance lies in comprehending the values of true positives, true negatives, false positives, and false negatives within the specific application context [51]. For example, false positives could result in the exoskeleton being activated during rest periods, which might be inconvenient or uncomfortable for the user. On the other hand, false negatives could mean that the exoskeleton fails to provide assistance when needed during walking activities. Having a higher number of true

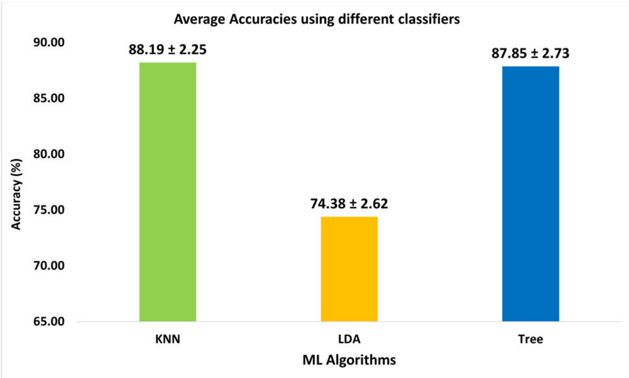

FIGURE 6. Average classification accuracies using different machine learning algorithms.

positives and true negatives in the confusion matrix is very important because it shows that the model is performing well in accurately identifying both classes. Fig. 7 provides a confusion matrix for two different subjects. It can be observed that for both subjects there are significantly higher numbers of true positive and true negative. In terms of controlling the lower limb exoskeleton, this means that the model is reliable in activating the exoskeleton while walking and not activating it during rest periods. This positive outcome ensures that the exoskeleton responds appropriately during movement and remains inactive when it's not needed. This can contribute to user comfort, safety, and effective support during walking.

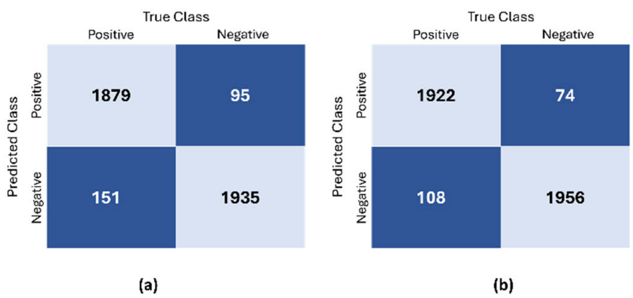

FIGURE 7. (a) Confusion Matrix of Subject 2; (b) Confusion Matrix of Subject 18.

For further analysis of the most optimal classifier, F1 score, recall, and precision were examined for each subject. Among all three measures, kNN demonstrated superior performance with values of 0.926, 0.933, and 0.920 respectively. In the context of this study, the importance of precision, recall, and F1 score relies on the specific priorities of the application [52]. If it is crucial to prevent unnecessary activation of the exoskeleton while at rest, then precision becomes more significant. On the other hand, if ensuring that the exoskeleton activates when needed during walking is a priority, then recall might hold greater importance. The F1 score offers a balanced assessment when both precision and recall are equally important considerations. In this case, precision is more important because it is imperative to avoid activating the lower limb exoskeleton when the user is in the rest position. Table 2 displays the F1 score, recall, and precision for each classifier

TABLE 2. Subject-wise evaluation matrices.

Participants		KNN	LDA	Tree
Subject 1	Precision	0.911	0.822	0.912
	Recall	0.929	0.710	0.914
	F1 Score	0.920	0.762	0.913
Subject 2	Precision	0.952	0.888	0.956
	Recall	0.926	0.892	0.959
	F1 Score	0.939	0.890	0.957
Subject 3	Precision	0.950	0.892	0.953
	Recall	0.976	0.774	0.949
	F1 Score	0.963	0.829	0.951
Subject 4	Precision	0.881	0.671	0.913
	Recall	0.944	0.727	0.920
	F1 Score	0.911	0.698	0.917
Subject 5	Precision	0.973	0.646	0.945
	Recall	0.948	0.579	0.940
	F1 Score	0.960	0.611	0.942
Subject 6	Precision	0.887	0.703	0.895
	Recall	0.941	0.709	0.902
	F1 Score	0.913	0.706	0.898
Subject 7	Precision	0.895	0.795	0.940
	Recall	0.961	0.802	0.944
	F1 Score	0.927	0.798	0.942
Subject 8	Precision	0.928	0.771	0.930
	Recall	0.927	0.777	0.924
	F1 Score	0.927	0.774	0.927
Subject 9	Precision	0.914	0.761	0.931
	Recall	0.965	0.776	0.922
	F1 Score	0.939	0.769	0.927
Subject 10	Precision	0.955	0.896	0.968
	Recall	0.973	0.923	0.967
	F1 Score	0.964	0.909	0.968
Subject 11	Precision	0.903	0.716	0.887
	Recall	0.840	0.699	0.890
	F1 Score	0.870	0.708	0.889
Subject 12	Precision	0.926	0.824	0.931
	Recall	0.953	0.896	0.930
	F1 Score	0.940	0.858	0.930
Subject 13	Precision	0.912	0.710	0.922
	Recall	0.918	0.839	0.918
	F1 Score	0.915	0.769	0.920
Subject 14	Precision	0.822	0.631	0.884
	Recall	0.829	0.727	0.887
	F1 Score	0.826	0.676	0.885
Subject 15	Precision	0.933	0.836	0.939
	Recall	0.954	0.816	0.951
	F1 Score	0.943	0.826	0.945
Subject 16	Precision	0.941	0.799	0.915
	Recall	0.935	0.815	0.917
	F1 Score	0.938	0.807	0.916
Subject 17	Precision	0.897	0.800	0.937
	Recall	0.941	0.812	0.935
	F1 Score	0.919	0.806	0.936
Subject 18	Precision	0.963	0.840	0.975
	Recall	0.947	0.814	0.970

TABLE 2. ***(Continued.)*** **Subject-wise evaluation matrices.**

	F1 Score	0.955	0.827	0.973
Subject 19	Precision	0.923	0.771	0.955
	Recall	0.938	0.749	0.954
	F1 Score	0.931	0.760	0.954
Subject 20	Precision	0.928	0.705	0.907
	Recall	0.925	0.605	0.908
	F1 Score	0.926	0.651	0.908
Average	**Precision**	**0.920±0.33**	**0.774±0.078**	**0.930±0.025**

across different subjects followed by a visual representation in Fig. 8.

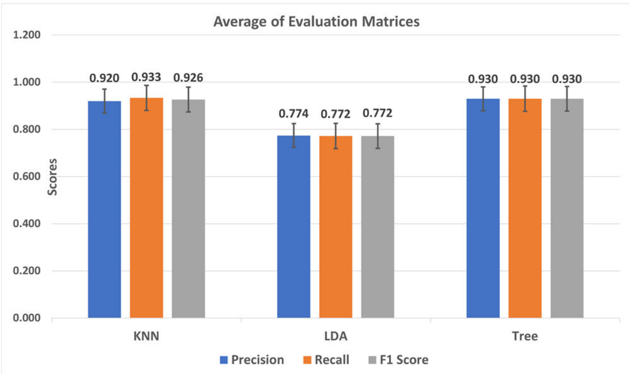

FIGURE 8. **Average of evaluation matrices.**

B. SIMULATED ONLINE

The simulated online configuration resembles real-time configuration and was used to test proposed methodology in likewise real-time settings. The commands for control of an exoskeleton were generated in a simulated online configuration. In this configuration, pre-recorded and unseen trials were fed to the classifier in a real-time manner. The simulated-online approach was applied solely to generate control commands using proposed BCI methodology to stop and trigger movement in exoskeleton.

The performance parameters of an exoskeleton leg can be evaluated based on how closely it imitates the movements of a natural leg. To do this, we can compare the walking patterns of humans with those of robotic legs. The effectiveness of rehabilitation for an individual with gait impairment can be evaluated by assessing their ability to replicate the movements of a healthy individual [53]. Gait analysis provides us with the kinematic parameters needed for modeling purposes. Fig. 9 represents the visual representation of BCI. In the field of BCI, the objective is to utilize signals from the brain to generate control commands. These signals undergo a four-stage process, involving preprocessing to eliminate any experimental noise, psychological noise or motion artifacts [54], extracting relevant data through feature extraction, classifying the data using different techniques and ultimately generating commands based on a trained model [7]. We have preprocessed the data, extracted suitable features, and obtained the optimal classification accuracies. Now we need to generate control commands for the lower limb exoskeleton. The commands for control of an exoskeleton were generated in a simulated online configuration. In this configuration, pre-recorded and unseen trials were fed to the classifier in a real-time manner.

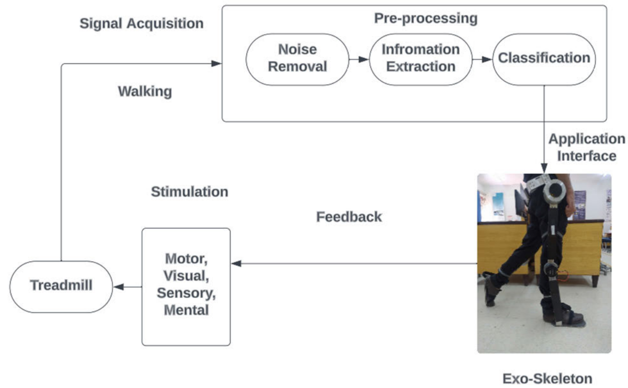

FIGURE 9. **General illustration of BCI.**

Attaining a seamless interface between the user and the rehabilitation device is a challenge [55], [56] which can be solved by windowing approach, it allows the exoskeleton to adapt seamlessly to the user's movements [24]. Sliding windowing technique [57] was implemented to extract the selected window as one sample, following the complete BCI pipeline to generate control command. fNIRS signal was sampled at 2.5 sec time window with 0.5 sec overlapping time. By utilizing a five-featured combination—mean, variance, skewness, kurtosis, and slope—extracted from each window, the fNIRS data was converted into binary control commands. Two control commands were used: 'Rest' to stop movement and 'Active' to trigger movement. The kNN classifier, carefully tuned to an optimal k-value [58], emerged as the preferred choice due to its significant accuracy in simulated-online BCI application as shown in Table 3. This study takes a step further in generation exoskeleton control commands in a simulated online configuration by implementing sliding windowing on fNIRS signal and utilizing a kNN classifier.

IV. DISCUSSION

The integration of BCI with robotic exoskeletons represents a significant advancement in the field of mobility assistance and rehabilitation. The findings of this study focused on the selection of appropriate features and classification algorithms for optimal control of exoskeletons. Through a comprehensive analysis, it was determined that a six-feature combination i.e. mean-variance-skewness-kurtosis-peak-slope yielded significantly better classification accuracies, with the kNN algorithm outperforming other classifiers. This highlights the critical role of feature selection and algorithm choice in achieving robust and accurate control of exoskeletons.

TABLE 3. Accuracies of 20 subjects for real-time bci using knn classifier.

Participants	Optimal K	Accuracy (%)
Subject 1	14	97.25
Subject 2	14	98.75
Subject 3	15	99.25
Subject 4	24	94.25
Subject 5	22	99.12
Subject 6	10	98.50
Subject 7	10	97.88
Subject 8	15	99.25
Subject 9	19	96.50
Subject 10	14	98.38
Subject 11	23	91.75
Subject 12	15	97.75
Subject 13	12	99.12
Subject 14	18	93.63
Subject 15	15	97.75
Subject 16	14	98.75
Subject 17	12	98.75
Subject 18	18	99.25
Subject 19	20	98.00
Subject 20	19	97.00
Average		**97.54**

Previously, a study conducted by García-Cossio et al. computed the classification accuracy of 83.4 $\pm$ 7.4% between passive and active walking during robotic-assisted treadmill walking using EEG modality [59]. Another study conducted on a lower-limb exoskeleton controlled by EEG signals for gait training showed an average accuracy of 80.16 $\pm$ 5.44% [60]. The classification accuracy using the LDA algorithm was 71.68% for controlling an exoskeleton rehabilitation robot based on motor imagery (MI) using EEG signals [61]. Research conducted by Khan et al. presented a novel fNIRS-BCI interface for controlling a prosthesis leg for gait rehabilitation and results showed an average accuracy of 75% using SVM for 9 subjects [39]. Another study presented the classification performance of fNIRS-BCI system for gait rehabilitation and achieved classification accuracy of 73.91% and 88.50% using kNN and convolutional neural networks (CNNs), respectively [62]. The kNN classifier achieved highest accuracy of 88.19 $\pm$ 2.55% which is significantly better than previous studies (i.e. 86.30%) conducted on BCI based lower extremity prosthesis and exoskeletons [63]. The confusion matrix revealed a high number of true positives and true negatives, indicating the model's effectiveness in activating the exoskeleton during walking and remaining inactive during rest periods. This ensures user comfort, safety, and targeted support. The high F1 score, precision, and recall further emphasize the model's ability to accurately distinguish between walking and rest states, prioritizing the prevention of unnecessary exoskeleton activation during rest.

Brain activation maps provided us with detailed insights into the specific regions of the brain that are active when gait activity is performed. Satori 2.0 software was utilized to visualize the changes in levels of oxygenated haemoglobin (ΔHbO). Brain images provide information about most activated regions of brain involved in coordinating movements during walking [64]. Sliding windowing was implemented for real-time analysis of fNIRS data. By dividing the fNIRS dataset into time windows and utilizing a kNN classifier, the study achieved seamless adaptation of the exoskeleton to the user's movements [65]. Selecting the suitable number of neighbors is important in the kNN algorithm's performance. The elbow method was employed to determine the optimal 'k' value. This was done by plotting the model's performance metrics, such as accuracy, across various 'k-nearest neighbors' values and identifying where the performance peaks. This optimal six feature combination allows the kNN algorithm to extract the most relevant information from the fNIRS data, leading to a more accurate distinction between walking and rest. Moreover, selection of optimal value of 'k' resulted in better classification accuracies of two-class data than previous studies. The sliding window approach allowed the system to analyze brain activity throughout the experiment allowing the real-time adaptation to change in gait patterns more effectively than previous methods.

The experimental paradigm is limited to only two classes i.e. rest and walking. A paradigm with different walking speeds or terrains might reveal more about brain activity during gait. Furthermore, conducting an analysis across various gait cycles could further enhance understanding of the neural activity in different brain regions. Implementation of the real-time control of exoskeleton can be done to evaluate its effectiveness in a real-world environment. Future research could involve individuals with varying degrees of mobility impairments that might affect gait patterns. This would provide detailed insight into the effectiveness of the fNIRS-BCI system for controlling exoskeletons. Future research could explore incorporating user feedback mechanisms to further personalize and optimize control strategies. It would be beneficial to investigate the potential of hybrid BCI modalities, such as EEG which might offer higher temporal resolution or different insights into brain activity during walking.

V. CONCLUSION

In this study, optimal feature combination, optimal classifier, and optimal k-nearest neighbors were analyzed and selected to improve the classification performance of fNIRS-BCI for gait rehabilitation. Six-feature combination of mean-peak-variance-skewness-kurtosis-slope was selected as optimal feature combination for classification. Similarly, kNN classification algorithm performed better as compared to LDA and Tree algorithms, with k-nearest neighbors estimated using elbow method. The proposed methodology attained enhanced performance of fNIRS-BCI system as compared to conventional methods and showed significantly ($p < 0.005$) better performance with achieved average classification accuracy of 88.19 $\pm$ 2.55 %. The simulated-online approach was applied to test proposed method in resemble to real-time settings. Windowing of 2.5 sec was used and achieved average classification accuracy of 97.54%. This provides improved intuitive control of exoskeleton for assistive and gait rehabilitation purposes.

ACKNOWLEDGMENT

This project has been partially supported by Gulf University for Science and Technology. The authors extend their gratitude to the researchers at Oslo Metropolitan University for granting access to the data analysis software. Additionally, they would also like to thank the National Centre of Robotics and Automation (NCRA).

REFERENCES

[1] H. Khan, N. Naseer, A. Yazidi, P. K. Eide, H. W. Hassan, and P. Mirtaheri, "Analysis of human gait using hybrid EEG-fNIRS-based BCI system: A review," *Frontiers Hum. Neurosci.*, vol. 14, Jan. 2021, Art. no. 613254, doi: 10.3389/fnhum.2020.613254.

[2] J. Schack, A. H. Pripp, P. Mirtaheri, H. Steen, E. Güler, and T. Gjøvaag, "Increased prefrontal cortical activation during challenging walking conditions in persons with lower limb amputation—An fNIRS observational study," *Physiotherapy Theory Pract.*, vol. 38, no. 2, pp. 255–265, Feb. 2022, doi: 10.1080/09593985.2020.1758979.

[3] H. Li, A. Gong, L. Zhao, F. Wang, Q. Qian, J. Zhou, and Y. Fu, "Identification of gait imagery based on fNIRS and class-dependent sparse representation," *Biomed. Signal Process. Control*, vol. 68, Jul. 2021, Art. no. 102597, doi: 10.1016/j.bspc.2021.102597.

[4] R. L. Hybart and D. P. Ferris, "Embodiment for robotic lower-limb exoskeletons: A narrative review," *IEEE Trans. Neural Syst. Rehabil. Eng.*, vol. 31, pp. 657–668, 2023, doi: 10.1109/TNSRE.2022.3229563.

[5] B. H. Dobkin, "Rehabilitation after stroke," *New England J. Med.*, vol. 352, no. 16, pp. 1677–1684, Apr. 2005, doi: 10.1056/nejmcp043511.

[6] I. Sinovas-Alonso, Á. Gil-Agudo, R. Cano-de-la-Cuerda, and A. J. del-Ama, "Walking ability outcome measures in individuals with spinal cord injury: A systematic review," *Int. J. Environ. Res. Public Health*, vol. 18, no. 18, p. 9517, Sep. 2021, doi: 10.3390/ijerph18189517.

[7] S. Peters, S. B. Lim, D. R. Louie, C.-L. Yang, and J. J. Eng, "Passive, yet not inactive: Robotic exoskeleton walking increases cortical activation dependent on task," *J. NeuroEng. Rehabil.*, vol. 17, no. 1, p. 107, Dec. 2020, doi: 10.1186/s12984-020-00739-6.

[8] N. Robinson, R. Mane, T. Chouhan, and C. Guan, "Emerging trends in BCI-robotics for motor control and rehabilitation," *Current Opinion Biomed. Eng.*, vol. 20, Dec. 2021, Art. no. 100354, doi: 10.1016/j.cobme.2021.100354.

[9] Z. Qi, W. Chen, J. Wang, J. Zhang, and X. Wang, "Lower limb rehabilitation exoskeleton control based on SSVEP-BCI," in *Proc. IEEE 16th Conf. Ind. Electron. Appl. (ICIEA)*, Aug. 2021, pp. 1954–1959, doi: 10.1109/ICIEA51954.2021.9516146.

[10] M. Alimardani and K. Hiraki, "Passive brain–computer interfaces for enhanced human–robot interaction," *Frontiers Robot. AI*, vol. 7, p. 125, Oct. 2020, doi: 10.3389/frobt.2020.00125.

[11] B. H. Dobkin, "Brain–computer interface technology as a tool to augment plasticity and outcomes for neurological rehabilitation," *J. Physiol.*, vol. 579, no. 3, pp. 637–642, Mar. 2007, doi: 10.1113/jphysiol.2006.123067.

[12] Z.-Z. Ma, J.-J. Wu, Z. Cao, X.-Y. Hua, M.-X. Zheng, X.-X. Xing, J. Ma, and J.-G. Xu, "Motor imagery-based brain–computer interface rehabilitation programs enhance upper extremity performance and cortical activation in stroke patients," *J. NeuroEng. Rehabil.*, vol. 21, no. 1, p. 91, May 2024, doi: 10.1186/s12984-024-01387-w.

[13] C. A. Cifuentes and M. Múnera, *Interfacing Humans and Robots for Gait Assistance and Rehabilitation*, 1st ed., Cham, Switzerland: Springer, 2022, doi: 10.1007/978-3-030-79630-3.

[14] A. Pino, N. Tovar, P. Barria, K. Baleta, M. Múnera, and C. A. Cifuentes, "Brain–computer interface for controlling lower-limb exoskeletons," in *Interfacing Humans and Robots for Gait Assistance and Rehabilitation*. Cham, Switzerland: Springer, 2022, pp. 237–258, doi: 10.1007/978-3-030-79630-3_9.

[15] U. Umar, H. S. Minhas, N. Naseer, H. Nazeer, S. Iqbal, and M. N. Ahmed, "Design and simulation of lower-limb exoskeleton to assist paraplegic people in walking," in *Proc. 8th Int. Conf. Control, Decis. Inf. Technol. (CoDIT)*, vol. 1, İstanbul, Turkey, May 2022, pp. 855–860, doi: 10.1109/CoDIT55151.2022.9804158.

[16] S. M. Hosni, S. B. Borgheai, J. McLinden, and Y. Shahriari, "An fNIRS-based motor imagery BCI for ALS: A subject-specific data-driven approach," *IEEE Trans. Neural Syst. Rehabil. Eng.*, vol. 28, no. 12, pp. 3063–3073, Dec. 2020, doi: 10.1109/TNSRE.2020.3038717.

[17] T. Yamada, S. Umeyama, and K. Matsuda, "Multidistance probe arrangement to eliminate artifacts in functional near-infrared spectroscopy," *J. Biomed. Opt.*, vol. 14, no. 6, 2009, Art. no. 064034, doi: 10.1117/1.3275469.

[18] L. Ferrero, M. Ortiz, V. Quiles, E. Iáñez, J. A. Flores, and J. M. Azorín, "Brain symmetry analysis during the use of a BCI based on motor imagery for the control of a lower-limb exoskeleton," *Symmetry*, vol. 13, no. 9, p. 1746, Sep. 2021, doi: 10.3390/sym13091746.

[19] A. Curtin, S. Tong, J. Sun, J. Wang, B. Onaral, and H. Ayaz, "A systematic review of integrated functional near-infrared spectroscopy (fNIRS) and transcranial magnetic stimulation (TMS) studies," *Frontiers Neurosci.*, vol. 13, p. 84, Feb. 2019, doi: 10.3389/fnins.2019.00084.

[20] R. A. Ramadan and A. V. Vasilakos, "Brain computer interface: Control signals review," *Neurocomputing*, vol. 223, pp. 26–44, Feb. 2017, doi: 10.1016/j.neucom.2016.10.024.

[21] P. Pinti, C. Aichelburg, S. Gilbert, A. Hamilton, J. Hirsch, P. Burgess, and I. Tachtsidis, "A review on the use of wearable functional near-infrared spectroscopy in naturalistic environments," *Jpn. Psychol. Res.*, vol. 60, no. 4, pp. 347–373, Oct. 2018, doi: 10.1111/jpr.12206.

[22] N. Naseer and K.-S. Hong, "FNIRS-based brain–computer interfaces: A review," *Frontiers Hum. Neurosci.*, vol. 9, p. 3, Jan. 2015, doi: 10.3389/fnhum.2015.00003.

[23] M. Tariq, P. M. Trivailo, and M. Simic, "EEG-based BCI control schemes for lower-limb assistive-robots," *Frontiers Hum. Neurosci.*, vol. 12, p. 312, Aug. 2018, doi: 10.3389/fnhum.2018.00312.

[24] P. Caliandro, F. Molteni, C. Simbolotti, E. Guanziroli, C. Iacovelli, G. Reale, S. Giovannini, and L. Padua, "Exoskeleton-assisted gait in chronic stroke: An EMG and functional near-infrared spectroscopy study of muscle activation patterns and prefrontal cortex activity," *Clin. Neurophysiol.*, vol. 131, no. 8, pp. 1775–1781, Aug. 2020, doi: 10.1016/j.clinph.2020.04.158.

[25] H. Nazeer and N. Naseer, "Brain-controlled lower-limb exoskeleton to assist elderly and disabled," in *Proc. 8th Int. Conf. Control, Decis. Inf. Technol. (CoDIT)*, vol. 1, May 2022, pp. 827–830, doi: 10.1109/CoDIT55151.2022.9804050.

[26] N. Naseer and K.-S. Hong, "Classification of functional near-infrared spectroscopy signals corresponding to the right- and left-wrist motor imagery for development of a brain–computer interface," *Neurosci. Lett.*, vol. 553, pp. 84–89, Oct. 2013, doi: 10.1016/j.neulet.2013.08.021.

[27] P. H. S. Pelicioni, M. Tijsma, S. R. Lord, and J. Menant, "Prefrontal cortical activation measured by fNIRS during walking: Effects of age, disease and secondary task," *PeerJ*, vol. 7, May 2019, Art. no. e6833, doi: 10.7717/peerj.6833.

[28] World Medical Association, "World Medical Association declaration of Helsinki. Ethical principles for medical research involving human subjects," *J. Amer. Med. Assoc.*, vol. 310, no. 20, pp. 2191–2194, Nov. 2013, doi: 10.1001/jama.2013.281053.

[29] H. Nazeer, N. Naseer, R. A. Khan, F. M. Noori, N. K. Qureshi, U. S. Khan, and M. J. Khan, "Enhancing classification accuracy of fNIRS-BCI using features acquired from vector-based phase analysis," *J. Neural Eng.*, vol. 17, no. 5, Oct. 2020, Art. no. 056025, doi: 10.1088/1741-2552/abb417.

[30] L. Gagnon, M. A. Yücel, D. A. Boas, and R. J. Cooper, "Further improvement in reducing superficial contamination in NIRS using double short separation measurements," *NeuroImage*, vol. 85, pp. 127–135, Jan. 2014, doi: 10.1016/j.neuroimage.2013.01.073.

[31] J. Kwasa, H. M. Peterson, K. Karrobi, L. Jones, T. Parker, N. Nickerson, and S. Wood, "Demographic reporting and phenotypic exclusion in fNIRS," *Frontiers Neurosci.*, vol. 17, May 2023, Art. no. 1086208, doi: 10.3389/fnins.2023.1086208.

[32] R. Dale, T. D. O'Sullivan, S. Howard, F. Orihuela-Espina, and H. Dehghani, "System derived spatial–temporal CNN for high-density fNIRS BCI," *IEEE Open J. Eng. Med. Biol.*, vol. 4, pp. 85–95, 2023, doi: 10.1109/OJEMB.2023.3248492.

[33] R. W. Homan, J. Herman, and P. Purdy, "Cerebral location of international 10–20 system electrode placement," *Electroencephalogr. Clin. Neurophysiol.*, vol. 66, no. 4, pp. 376–382, Apr. 1987, doi: 10.1016/0013-4694(87)90206-9.

[34] K. Jezierska, A. Sękowska-Namiotko, B. Pala, D. Lietz-Kijak, H. Gronwald, and W. Podraza, "Searching for the mechanism of action of extremely low frequency electromagnetic field—The pilot fNIRS research," *Int. J. Environ. Res. Public Health*, vol. 19, no. 7, p. 4012, Mar. 2022, doi: 10.3390/ijerph19074012.

[35] J. Bonnal, F. Monnet, B.-T. Le, O. Pila, A.-G. Grosmaire, C. Ozsancak, C. Duret, and P. Auzou, ''Relation between cortical activation and effort during robot-mediated walking in healthy people: A functional near-infrared spectroscopy neuroimaging study (fNIRS),'' *Sensors*, vol. 22, no. 15, p. 5542, Jul. 2022, doi: 10.3390/s22155542.

[36] N. Hakimi, M. Shahbakhti, J. M. Horschig, T. Alderliesten, F. Van Bel, W. N. J. M. Colier, and J. Dudink, ''Respiratory rate extraction from neonatal near-infrared spectroscopy signals,'' *Sensors*, vol. 23, no. 9, p. 4487, May 2023, doi: 10.3390/s23094487.

[37] R. A. Khan, N. Naseer, S. Saleem, N. K. Qureshi, F. M. Noori, and M. J. Khan, ''Cortical tasks-based optimal filter selection: An fNIRS study,'' *J. Healthcare Eng.*, vol. 2020, pp. 1–15, May 2020, doi: 10.1155/2020/9152369.

[38] P. W. Dans, S. D. Foglia, and A. J. Nelson, ''Data processing in functional near-infrared spectroscopy (fNIRS) motor control research,'' *Brain Sci.*, vol. 11, no. 5, p. 606, May 2021, doi: 10.3390/brainsci11050606.

[39] R. A. Khan, N. Naseer, N. K. Qureshi, F. M. Noori, H. Nazeer, and M. U. Khan, ''FNIRS-based neurorobotic interface for gait rehabilitation,'' *J. NeuroEng. Rehabil.*, vol. 15, no. 1, p. 7, Dec. 2018, doi: 10.1186/s12984-018-0346-2.

[40] L. Kocsis, P. Herman, and A. Eke, ''The modified Beer–Lambert law revisited,'' *Phys. Med. Biol.*, vol. 51, no. 5, pp. N91–N98, Mar. 2006, doi: 10.1088/0031-9155/51/5/n02.

[41] A. Janani and M. Sasikala, ''Investigation of different approaches for noise reduction in functional near-infrared spectroscopy signals for brain–computer interface applications,'' *Neural Comput. Appl.*, vol. 28, no. 10, pp. 2889–2903, Oct. 2017, doi: 10.1007/s00521-017-2961-4.

[42] M. Zhao, G. Bonassi, J. Samogin, G. A. Taberna, E. Pelosin, A. Nieuwboer, L. Avanzino, and D. Mantini, ''Frequency-dependent modulation of neural oscillations across the gait cycle,'' *Hum. Brain Mapping*, vol. 43, no. 11, pp. 3404–3415, Aug. 2022, doi: 10.1002/hbm.25856.

[43] V. Marchal, J. Sellers, M. Pélégrini-Issac, C. Galléa, E. Bertasi, R. Valabrègue, B. Lau, P. Leboucher, E. Bardinet, M.-L. Welter, and C. Karachi, ''Deep brain activation patterns involved in virtual gait without and with a doorway: An fMRI study,'' *PLoS ONE*, vol. 14, no. 10, Oct. 2019, Art. no. e0223494, doi: 10.1371/journal.pone.0223494.

[44] A. M. Batula, J. A. Mark, Y. E. Kim, and H. Ayaz, ''Comparison of brain activation during motor imagery and motor movement using fNIRS,'' *Comput. Intell. Neurosci.*, vol. 2017, no. 1, pp. 1–12, 2017, doi: 10.1155/2017/5491296.

[45] A. von Lühmann, A. Ortega-Martinez, D. A. Boas, and M. A. Yücel, ''Using the general linear model to improve performance in fNIRS single trial analysis and classification: A perspective,'' *Frontiers Hum. Neurosci.*, vol. 14, p. 30, Feb. 2020, doi: 10.3389/fnhum.2020.00030.

[46] S. Zhang, X. Li, M. Zong, X. Zhu, and R. Wang, ''Efficient kNN classification with different numbers of nearest neighbors,'' *IEEE Trans. Neural Netw. Learn. Syst.*, vol. 29, no. 5, pp. 1774–1785, May 2018, doi: 10.1109/TNNLS.2017.2673241.

[47] S. Zhang, X. Li, M. Zong, X. Zhu, and D. Cheng, ''Learning k for kNN classification,'' *ACM Trans. Intell. Syst. Technol.*, vol. 8, no. 3, pp. 1–19, May 2017, doi: 10.1145/2990508.

[48] S. Ougiaroglou and G. Evangelidis, ''Dealing with noisy data in the context of k-NN classification,'' in *Proc. 7th Balkan Conf. Informat. Conf.*, New York, NY, USA, Sep. 2015, pp. 1–4, doi: 10.1145/2801081.2801116.

[49] F. Sutomo, D. A. Muaafii, D. N. Al Rasyid, Y. I. Kurniawan, L. Afuan, T. Cahyono, E. Maryanto, and D. Iskandar, ''Optimization of the k-nearest neighbors algorithm using the elbow method on stroke prediction,'' *Jurnal Teknik Informatika*, vol. 4, no. 1, pp. 125–130, Feb. 2023, doi: 10.52436/1.jutif.2023.4.1.839.

[50] S. Tak and J. C. Ye, ''Statistical analysis of fNIRS data: A comprehensive review,'' *NeuroImage*, vol. 85, pp. 72–91, Jan. 2014, doi: 10.1016/j.neuroimage.2013.06.016.

[51] T. Ma, S. Wang, Y. Xia, X. Zhu, J. Evans, Y. Sun, and S. He, ''CNN-based classification of fNIRS signals in motor imagery BCI system,'' *J. Neural Eng.*, vol. 18, no. 5, Oct. 2021, Art. no. 056019, doi: 10.1088/1741-2552/abf187.

[52] S. Karmakar, S. Kamilya, P. Dey, P. K. Guhathakurta, M. Dalui, T. K. Bera, S. Halder, C. Koley, T. Pal, and A. Basu, ''Real time detection of cognitive load using fNIRS: A deep learning approach,'' *Biomed. Signal Process. Control*, vol. 80, Feb. 2023, Art. no. 104227, doi: 10.1016/j.bspc.2022.104227.

[53] U. Asgher, M. J. Khan, M. H. Asif Nizami, K. Khalil, R. Ahmad, Y. Ayaz, and N. Naseer, ''Motor training using mental workload (MWL) with an assistive soft exoskeleton system: A functional near-infrared spectroscopy (fNIRS) study for brain–machine interface (BMI),'' *Frontiers Neurorobot.*, vol. 15, Mar. 2021, Art. no. 605751, doi: 10.3389/fnbot.2021.605751.

[54] S. L. Novi, E. Roberts, D. Spagnuolo, B. M. Spilsbury, D. C. Price, C. A. Imbalzano, E. Forero, A. G. Yodh, G. M. Tellis, C. M. Tellis, and R. C. Mesquita, ''Functional near-infrared spectroscopy for speech protocols: Characterization of motion artifacts and guidelines for improving data analysis,'' *Proc. SPIE*, vol. 7, no. 1, Jan. 2020, Art. no. 015001, doi: 10.1117/1.nph.7.1.015001.

[55] R. Mendoza-Crespo, D. Torricelli, J. C. Huegel, J. L. Gordillo, J. L. Pons, and R. Soto, ''An adaptable human-like gait pattern generator derived from a lower limb exoskeleton,'' *Frontiers Robot. AI*, vol. 6, p. 36, May 2019, doi: 10.3389/frobt.2019.00036.

[56] K. K. Karunakaran, K. Abbruzzese, G. Androwis, and R. A. Foulds, ''A novel user control for lower extremity rehabilitation exoskeletons,'' *Frontiers Robot. AI*, vol. 7, p. 108, Sep. 2020, doi: 10.3389/frobt.2020.00108.

[57] Y. Oda, T. Sato, I. Nambu, and Y. Wada, ''Real-time reduction of task-related scalp-hemodynamics artifact in functional near-infrared spectroscopy with sliding-window analysis,'' *Appl. Sci.*, vol. 8, no. 1, p. 149, Jan. 2018, doi: 10.3390/app8010149.

[58] R. Shetty, M. Geetha, D. U. Acharya, and G. Shyamala, ''Data preprocessing and finding optimal value of K for KNN model,'' in *Soft Computing and Signal Processing* (Advances in Intelligent Systems and Computing). Singapore: Springer, 2021, pp. 1–9, doi: 10.1007/978-981-16-7088-6_1.

[59] E. García-Cossio, M. Severens, B. Nienhuis, J. Duysens, P. Desain, N. Keijsers, and J. Farquhar, ''Decoding sensorimotor rhythms during robotic-assisted treadmill walking for brain computer interface (BCI) applications,'' *PLoS ONE*, vol. 10, no. 12, Dec. 2015, Art. no. e0137910, doi: 10.1371/journal.pone.0137910.

[60] D. Liu, W. Chen, Z. Pei, and J. Wang, ''A brain-controlled lower-limb exoskeleton for human gait training,'' *Rev. Sci. Instrum.*, vol. 88, no. 10, Oct. 2017, Art. no. 104302, doi: 10.1063/1.5006461.

[61] G. Yu, J. Wang, W. Chen, and J. Zhang, ''EEG-based brain-controlled lower extremity exoskeleton rehabilitation robot,'' in *Proc. IEEE Int. Conf. Cybern. Intell. Syst. (CIS), IEEE Conf. Robot., Autom. Mechatronics (RAM)*, Ningbo, China, Nov. 2017, pp. 763–767, doi: 10.1109/ICCIS.2017.8274875.

[62] H. Hamid, N. Naseer, H. Nazeer, M. J. Khan, R. A. Khan, and U. S. Khan, ''Analyzing classification performance of fNIRS-BCI for gait rehabilitation using deep neural networks,'' *Sensors*, vol. 22, no. 5, p. 1932, Mar. 2022, doi: 10.3390/s22051932.

[63] A. H. Do, P. T. Wang, C. E. King, S. N. Chun, and Z. Nenadic, ''Brain–computer interface controlled robotic gait orthosis,'' *J. NeuroEng. Rehabil.*, vol. 10, no. 1, p. 111, 2013, doi: 10.1186/1743-0003-10-111.

[64] S. Tortora, L. Tonin, S. Sieghartsleitner, R. Ortner, C. Guger, O. Lennon, D. Coyle, E. Menegatti, and A. Del Felice, ''Effect of lower limb exoskeleton on the modulation of neural activity and gait classification,'' *IEEE Trans. Neural Syst. Rehabil. Eng.*, vol. 31, pp. 2988–3003, 2023, doi: 10.1109/TNSRE.2023.3294435.

[65] J. de Miguel-Fernández, J. Lobo-Prat, E. Prinsen, J. M. Font-Llagunes, and L. Marchal-Crespo, ''Control strategies used in lower limb exoskeletons for gait rehabilitation after brain injury: A systematic review and analysis of clinical effectiveness,'' *J. NeuroEng. Rehabil.*, vol. 20, no. 1, p. 23, Feb. 2023, doi: 10.1186/s12984-023-01144-5.

HAMZA SHABBIR MINHAS received the bachelor's degree in mechanical engineering from the University of Engineering and Technology (UET), Taxila, in 2019. He is currently a Lab Engineer with the Department of Mechatronics and Biomedical Engineering, Air University, Islamabad. His research interests include brain–computer interface, artificial intelligence, machine learning, and rehabilitation.

HAMMAD NAZEER (Senior Member, IEEE) received the bachelor's and master's degrees in mechatronics engineering from the National University of Science and Technology (NUST), and the Ph.D. degree in mechatronics engineering from Air University, Islamabad. He is currently an Assistant Professor with the Department of Mechatronics and Biomedical Engineering, Air University. He has published more than 15 peer-reviewed research articles. His research interests include robotic rehabilitation, brain–computer interface, mechatronics, neurorobotics, artificial intelligence, and machine learning.

NOMAN NASEER (Senior Member, IEEE) received the bachelor's degree from the E&ME College, NUST, Rawalpindi, the master's degree from Air University, Islamabad, Pakistan, and the Ph.D. degree in mechatronics engineering from Pusan National University, Seoul, South Korea.

He is currently a Tenured Associate Professor, the Chair of the Department of Mechatronics and Biomedical Engineering, and the Head of the Neurorobotics Research Group, Air University. He has published more than 83 peer-reviewed articles. His research interests include robotic rehabilitation, bio robotics, neurorobotics, artificial intelligence, and machine learning.

Dr. Naseer has been serving as an editorial board member for five SCI €-indexed journals. He is the Vice President of the IEEE Robotics and Automation Society. He served as a reviewer for above 80 SCI €-indexed journals.

UMAR SHAHBAZ KHAN (Member, IEEE) received the bachelor's degree in mechatronics engineering from the National University of Sciences and Technology, Pakistan, in 2005, and the Ph.D. degree in electrical engineering from the University of Liverpool, U.K., in 2010.

He is currently the Central Project Director of the National Center of Robotics and Automation (NCRA) and a Tenured Associate Professor with the E&ME College, NUST. He is also involved in the field of robotics and mainly toward the development of myo-electric controlled prosthesis. His research interests include robotics, mechatronics, embedded systems, and image processing.

ALI R. ANSARI is a Professor at the Gulf University for Science and Technology and has an academic with over 30 years' experience in teaching and research in the area of applied mathematics. He was the Dean of the College of Arts and Sciences, Gulf University for Science and Technology, Kuwait, for ten years. He is currently a Professor of applied mathematics and the Head of the Accreditation and Quality Assurance. He has more than 100 publications in the area of applied mathematics.

RAHEEL NAWAZ is an international thought leader in higher education and industry-academia co-design, who has advised national governments, policy organizations, and parliamentary committees on AI, digital education, and work-based learning. At Staffordshire University, he leads transformative action across the university to deliver an enhanced academic experience. With four books and over 200 research articles, he ranks among the top-10 most cited scholars in the world in the fields of applied AI, digital education, educational data science, and digital transformations.

Prof. Nawaz's sector-leading work on pedagogical design and delivery led to outstanding student outcomes, with first generation university students with minimal prior attainment outperforming graduates of top U.K. universities (including Oxbridge) in both average salaries and job security; he was awarded the National Teaching Fellowship (NTF) for this work. He has advised on the establishment and launch of work-based learning degree programs across three continents and received the Principal Fellowship of the Higher Education Academy (PFHEA) for this work. The impact of his academic leadership has been endorsed by heads of state, government ministers, and industry leaders. He passionately believes that kindness in the most impactful leadership trait and being an intrinsic giver in life is the most sustainable route to happiness, as outlined in his TEDx talk.